Effects of Vertical Wind Shear and Storm Motion on Tropical Cyclone Rainfall Asymmetries Deduced from TRMM

SHUYI S. CHEN

Rosenstiel School of Marine and Atmospheric Science, University of Miami, Miami, Florida

JOHN A. KNAFF

Cooperative Institute for Research in the Atmosphere, Colorado State University, Fort Collins, Colorado

FRANK D. MARKS JR.

NOAA/AOML/Hurricane Research Division, Miami, Florida

(Manuscript received 1 February 2005, in final form 2 February 2006)

ABSTRACT

Vertical wind shear and storm motion are two of the most important factors contributing to rainfall asymmetries in tropical cyclones (TCs). Global TC rainfall structure, in terms of azimuthal distribution and asymmetries relative to storm motion, has been previously described using the Tropical Rainfall Measuring Mission Microwave Imager rainfall estimates. The mean TC rainfall distribution and the wavenumber-1 asymmetry vary with storm intensity and geographical location among the six oceanic basins. This study uses a similar approach to investigate the relationship between the structure of TC rainfall and the environmental flow by computing the rainfall asymmetry relative to the vertical wind shear. The environmental vertical wind shear is defined as the difference between the mean wind vectors of the 200- and 850-hPa levels over an outer region extending from the radius of 200–800 km around the storm center. The wavenumber-1 maximum rainfall asymmetry is downshear left (right) in the Northern (Southern) Hemisphere. The rainfall asymmetry decreases (increases) with storm intensity (shear strength). The rainfall asymmetry maximum is predominantly downshear left for shear values > 7.5 m s^{-1}. Large asymmetries are usually observed away from the TC centers. As TC intensity increases, the asymmetry maximum shifts upwind to the left. The analysis is further extended to examine the storm motion and the vertical wind shear and their collective effects on TC rainfall asymmetries. It is found that the vertical wind shear is a dominant factor for the rainfall asymmetry when shear is >5 m s^{-1}. The storm motion–relative rainfall asymmetry in the outer rainband region is comparable to that of shear relative when the shear is <5 m s^{-1}, suggesting that TC translation speed becomes an important factor in the low shear environment. The overall TC rainfall asymmetry depends on the juxtaposition and relative magnitude of the storm motion and environmental shear vectors in all oceanic basins.

1. Introduction

Spatial distribution of rainfall in tropical cyclones (TCs) is of particular interest for the quantitative precipitation forecast (QPF). The TC rainfall can be described as the sum of an azimuthal average (or wavenumber 0) and a series of low-order wavenumbers (e.g., Marks et al. 1992; Lonfat et al. 2004, hereafter LMC). Although the rainfall accounted for by the wavenumber 0 tends to be dominant on average, a significant spatial variability in rainfall can be induced by various dynamic and thermodynamic processes in a TC. Previous studies have found that asymmetries in TC circulations are related to the gradient of planetary vorticity (Peng and Williams 1990; Bender 1997), the friction-induced asymmetric boundary layer convergence in a moving storm (e.g., Shapiro 1983), the existence of a mean flow across a TC (e.g., Bender 1997; Peng et al. 1999), the environmental vertical wind shear (Merrill 1988; Jones 1995, 2000a,b, 2004; DeMaria 1996; Frank and Ritchie 1999, 2001), and possibly the asymmetric moisture dis-

Corresponding author address: Dr. Shuyi S. Chen, RSMAS, University of Miami, 4600 Rickenbacker Causeway, Miami, FL 33149.
E-mail: schen@rsmas.miami.edu

tribution surrounding a storm (Dunion and Velden 2004).

The question is whether and how the asymmetry in TC circulations affects the spatial distribution of TC rainfall. LMC documented the global distribution of rainfall in TCs using satellite data from the Tropical Rainfall Measuring Mission (TRMM). They showed the mean characteristics of the TC rainfall and its asymmetry relative to storm motion, as a function of TC intensity, in six oceanic basins around the globe. Significant variability was found in the observed TC rainfall, which could not be fully explained by the global variability in TC intensity and motion from basin to basin.

In this paper, we examine the spatial distribution of TC rainfall and its relationship to the environmental flow with a focus on vertical wind shear. The shear-relative rainfall asymmetry will be compared with that relative to storm motion described in LMC. The TC motion is largely determined by the so-called steering flow that is commonly defined by a tropospheric mean circulation. However, the vertical wind shear can affect the steering flow. Although composites of shear-relative and motion-relative rainfall asymmetries are not totally independent, differences between them indicate two distinct processes may be contributing to the rainfall asymmetry. We will further examine the combined effects of storm motion and vertical wind shear on the observed TC rainfall asymmetry over the global oceans.

Rogers et al. (2003) examined rainfall asymmetry associated with vertical wind shear and storm motion in Hurricane Bonnie (in 1998) using a high-resolution, cloud-resolving model simulation. They found that the combination of shear and storm motion is critical in explaining the rainfall asymmetry in Bonnie. An along-track shear resulted in a symmetric rainfall accumulation before Bonnie recurved northward, whereas a cross-track shear created a right-side asymmetry in the accumulated rainfall as Bonnie approached the U.S. east coast.

Corbosiero and Molinari (2003) examined the spatial distribution of lightning in Atlantic hurricanes using data from the National Lightning Detection Network (NLDN) near the coastal regions. They observed a maximum occurrence of lightning downshear left. They also found that the vertical wind shear vector was to the right of the storm motion direction for most recurving storms near the U.S. east coast, similar to the cross-track shear in Hurricane Bonnie (in 1998) described by Rogers et al. (2003). Corbosiero and Molinari showed that the environmental shear is a dominant factor modulating the convective activity in hurricanes.

Vertical wind shear plays an important role in TC dynamics and evolution. Strong vertical wind shears can restrain TCs from reaching their maximum potential intensity (MPI; Emanuel 1988, 1997; Holland 1997). As a result, the environmental shear is considered as a key parameter in the operational TC intensity forecasts (e.g., Dvorak 1984; DeMaria and Kaplan 1994, 1999; Knaff et al. 2004, 2005). The importance of shear on the TC rainfall structure has not been examined extensively, aside from a few excellent case studies (e.g., Black et al. 2002), partly because of the lack of quantitative measurements of TC rainfall and environmental wind shear over the open ocean.

A number of numerical modeling studies have focused on the effect of vertical wind shear on TC structure and intensity (Jones 1995, 2000a,b, 2004; DeMaria 1996; Frank and Ritchie 1999, 2001). Although the level of complexity of the models varied, they all used an idealized symmetric vortex in a sheared environment. The evolution of the vortex was affected significantly by the direction and magnitude of the shear. Frank and Ritchie (2001) found that the vortex developed a wavenumber-1 asymmetry in vertical motion, cloud water, and precipitation fields in their idealized simulations when the vertical wind shear was introduced in the model. The asymmetry first occurred at the top of the vortex and propagated downward to the surface. The effect of shear became particularly pronounced when shear > 10 m s^{-1}.

The effect of storm motion on TC rainfall asymmetry has been documented in various observational studies (e.g., Miller 1958; Frank 1977; Marks 1985; Burpee and Black 1989; Rodgers et al. 1994; LMC). Rainfall is generally observed to have a maximum ahead of the TC center, which indicates the importance of surface friction–induced low-level convergence. However, the magnitude and the exact location of the rainfall asymmetry vary from storm to storm. Composites of storm motion–relative rainfall asymmetry of different oceanic basins by LMC showed a general front-to-back asymmetry.

The previous observational and modeling studies provide some evidence of the effects of environmental shear and storm motion on TC asymmetry in terms of storm structure and rainfall over the Atlantic or in idealized conditions. The generality and complexity of the TC rainfall asymmetry over the global oceans will be investigated in this study. We will use the TRMM rainfall observations, the vertical wind shear data (described in the next section), and the TC motion from the National Hurricane Center and the Joint Typhoon Warning Center best-track data to examine the relationship between the storm motion, environmental vertical wind shear, and TC rainfall asymmetry. We will also investigate how these relationships vary for differ-

ent TC intensity groups and over various oceanic basins.

2. Data and analyses

a. TRMM rainfall estimates

A description of the satellite instruments and frequencies on board TRMM can be found in Kummerow et al. (1998). In this study we use the TRMM Microwave Imager (TMI) and Precipitation Radar (PR) rainfall data from 1998 to 2000, which is the same time period used in LMC. The use of the same time period allows us to compare directly with results of LMC in which TC motion–relative rainfall analysis was presented. The TMI and PR footprints are 5×5 and 4×4 km, respectively. The dataset is partitioned into six oceanic basins defined in LMC (see Fig. 1 of LMC). Furthermore, the TC intensity groups, including the tropical storms (TSs), category 1–2 storms (CAT12), and category 3–5 storms (CAT35), are defined exactly the same as in LMC.

b. Vertical wind shear

The vertical wind shear is computed globally using the developmental datasets from the Statistical Hurricane Intensity Prediction Scheme (SHIPS; DeMaria and Kaplan 1999) and the Statistical Typhoon Intensity Prediction Scheme (STIPS; Knaff et al. 2005). The environmental vertical wind shear used in this study is defined as the difference between the 200- and 800-hPa ($V_{200} - V_{850}$) winds in an annular region between 200 and 800 km radii from the TC center, at 12-hourly time intervals. The TC positions are from the best-track datasets available from the National Hurricane Center (NHC; Jarvinen et al. 1984) and the Joint Typhoon Warning Center (JTWC; available online at https://metoc.npmoc.navy.mil/jtwc/best_tracks/). The National Centers for Environmental Prediction (NCEP) operational global analyses were used to compute the vertical wind shear in the Atlantic and eastern Pacific and the Navy Operational Global Analysis and Prediction System (NOGAPS; Hogan and Rosmond 1991) was used for the western North Pacific, north Indian Ocean, and the Southern Hemisphere. Both of the global analysis fields have $1^\circ \times 1^\circ$ grid resolution.

This definition of the environmental vertical wind shear is somewhat arbitrary, and is mostly representative of the deep-tropospheric shear between the 200- and 850-hPa levels. Elsberry and Jefferies (1996) have shown that the effect of vertical wind shear on TC formation and intensity is complex and may be sensitive to the shear profile. They found that some TC formations are affected by a relative shallow layer of strong wind shear in the upper troposphere. However, the focus of this study is on the shear effects on TC rainfall asymmetry that seem to be dominated by the deep-tropospheric shear as indicated by numerical studies of Rogers et al. (2003) and Desflots and Chen (2004). It is also supported by the TRMM PR data as shown later in section 3d.

c. NCEP reanalysis wind data

To provide a global context for the TRMM-observed TC environment from 1998 to 2000, we use the NCEP reanalysis global wind data (Kalnay et al. 1996) as a large-scale background for the vertical wind shear and rainfall analyses. The vertical wind shear is again defined as the difference between the horizontal wind fields at the 200- and 850-hPa levels same as for SHIPS and STIPS. The grid resolution of the NCEP reanalysis data is $2.5^\circ \times 2.5^\circ$.

d. Shear-relative rainfall analysis

The spatial distribution of TC rainfall is analyzed using a Fourier decomposition relative to the shear vector orientation. The wind shear at each TRMM observation is determined by linear interpolation of the two SHIPS data times nearest to the TRMM observation time. The total number of TRMM observations used in this analysis is slightly smaller than that in LMC because of the lack of collocated shear data over some TRMM-observed TCs. Spatial asymmetries are created by binning rainfall estimates in 10-km-wide annuli centered on the TC from 0 to nearly 330 km in radius. The decomposition method is identical to that described in LMC. In this approach, the phase maximum represents the location of the highest probability of rainfall occurrence. We then normalize the amplitude of higher wavenumbers to the wavenumber 0 (azimuthal average). The TC rainfall asymmetry is composited relative to the vertical wind shear vector over each TRMM observation. The larger the asymmetry amplitude, the more variability in the spatial distribution of TC rainfall may be explained by the reference system (either the environmental shear relative or the TC motion relative). This approach can only characterize the relative importance of individual parameters. A numerical modeling study is currently under way to further investigate the various interactive physical processes that may explain the observed TC rainfall distribution.

3. Vertical wind shear and shear-relative rainfall asymmetry

a. Global vertical wind shear for 1998–2000

To provide a large-scale context for the shear-relative TC rainfall analysis of 1998–2000, we examine

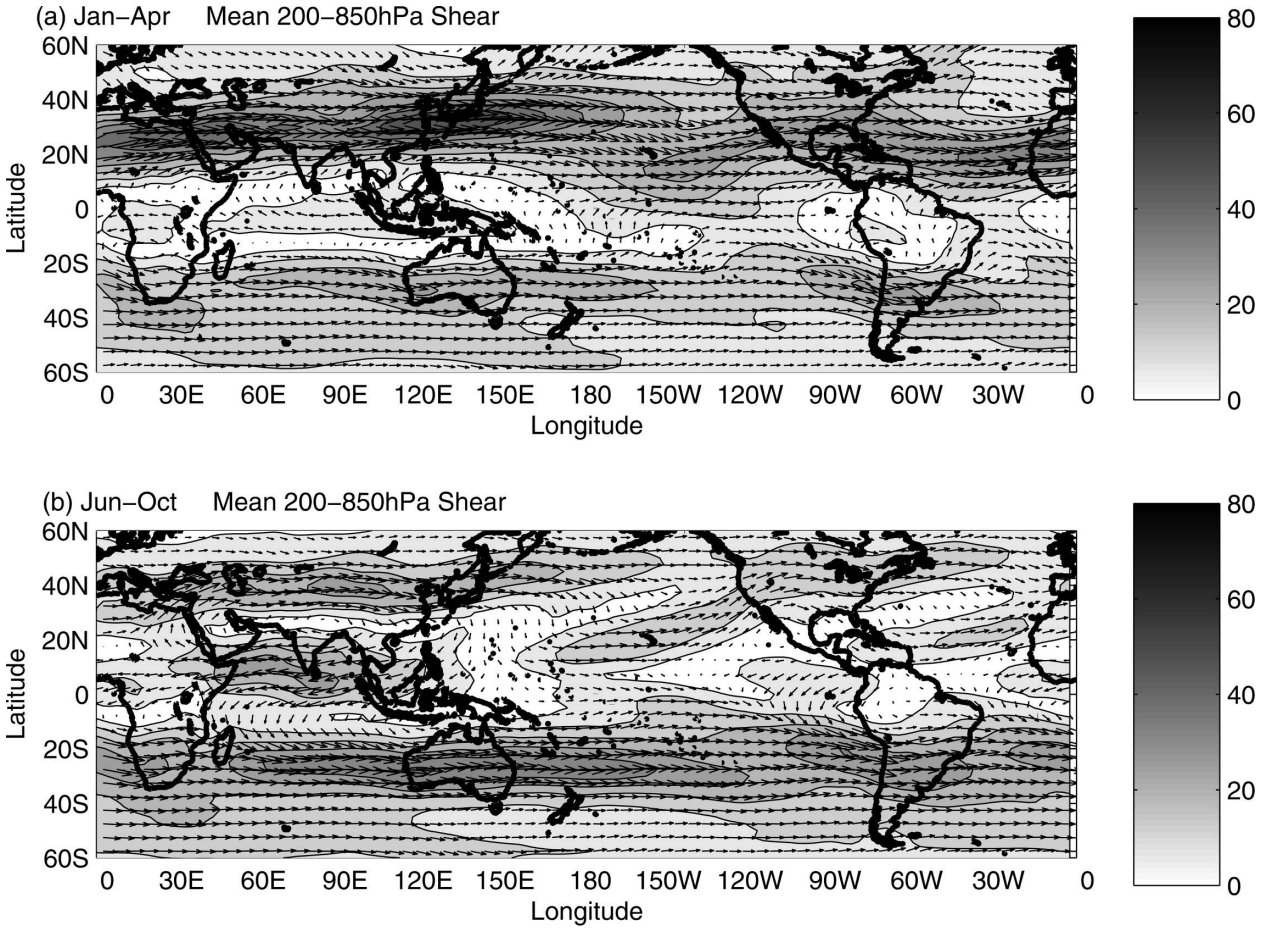

FIG. 1. Global mean vertical wind shear (grayscale in m s^{-1}, with contour intervals of 7.5 m s^{-1}) from the NCEP reanalysis wind data for the period of 1998–2000: (a) January–April and (b) June–October.

the global environmental vertical wind shear (Fig. 1) over various oceanic basins using the NCEP reanalysis. In the midlatitudes, westerly shear dominates in both NH and SH with the strongest shear during the winter season of each hemisphere. Within the Tropics, the shear is relatively weak, but the directional variability is large in comparison. During the austral summer, when the TCs are active in SH from January to April, the shear is mostly weak to moderate (<15 m s^{-1}) easterly over the south Indian (SIND) and South Pacific (SPAC) Oceans (Fig. 1a). During the boreal summer, when the TC activity is mostly in NH from June to October, the tropical northern Atlantic (ATL), the northern west Pacific (NWPAC), and the northern east Pacific (ECPAC) are dominated by relatively weak easterly shear, whereas the tropical northern Indian Ocean (NIND) is dominated by mean easterly shear (Fig. 1b). Although TCs tend to occur in relatively low shear environments, variability in vertical wind shear within the Tropics is evident from basin to basin. The shear varies from mostly 5 to 10 m s^{-1} or less between 10° and 20°S to above 15 m s^{-1} between 20° and 25°S latitude bands where TRMM-observed TCs are located over SIND and SPAC from January to April (Fig. 1a). The entire tropical North Pacific and Atlantic are under weak to moderate (<15 m s^{-1}) shear with the lowest shear in the west and east Pacific (<5–10 m s^{-1} in some areas) during the NH TC season from June to October. There is noticeable northerly shear component in NWPAC (Fig. 1b). The strongest shear (up to 25 m s^{-1}) is observed in NIND, especially near the southern tip of India, where the summer monsoon is dominant.

b. *Shear-relative rainfall asymmetry in different oceanic basins*

The vertical wind shear from SHIPS and STIPS over the corresponding TRMM observed TCs is shown in Fig. 2. Although the collocated data are relatively sparse, the general patterns and shear values are similar to that of seasonal mean in Fig. 1. A total of 424 ob-

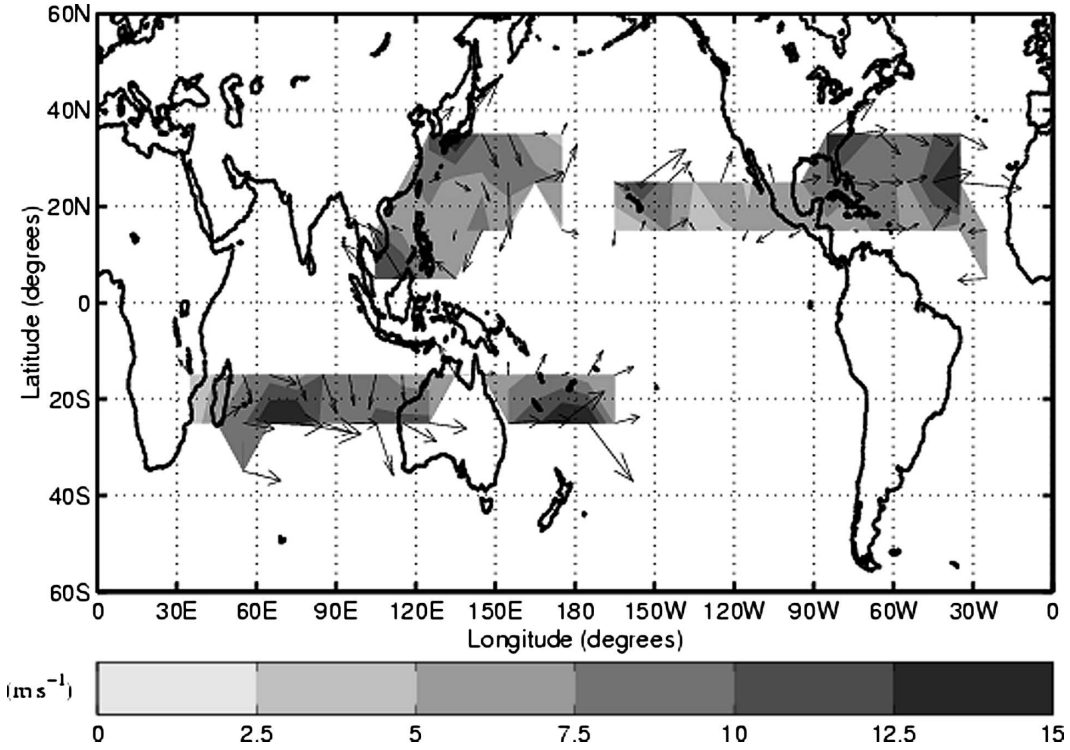

FIG. 2. The vertical wind shear from the SHIPS and STIPS dataset that is collocated with the TRMM TC observations during 1998–2000.

servations were obtained in ATL, 280 in ECPAC, 494 in NWPAC, 212 in SPAC, and 124 in SIND. The very small number of observations in NIND prevented the construction of a statistically significant result for that basin. The distribution of observations among basins is similar to that described in LMC. However, the ATL is sampled more frequently (by about 3%–4%) than in the original TC TRMM database and SIND is undersampled, by about 5%–6%.

Figure 3 presents the wavenumber-1 shear-relative rainfall asymmetry over the five oceanic basins. The asymmetry amplitude values shown in Fig. 3 (and in similar figures thereafter) are the fraction of the wavenumber 1 to the wavenumber 0 (azimuthal average). A value of 0.2 indicates that the wavenumber-1 asymmetry is 20% of the azimuthal mean value. The maximum wavenumber-1 rainfall asymmetry is clearly downshear left in the NH basins (Figs. 3a–c), especially in ATL and NWPAC. In the SH basins, as the Coriolis parameter changes sign from that in the NH, the maximum asymmetry is downshear right (Figs. 3d,e). In all oceanic basins, the location of the asymmetry maximum tends to shift upwind toward the shear direction as the distance from the center increases. In contrast, the amplitudes of the asymmetry have a large variability among the basins. The northern Pacific TCs are less asymmetric on average, with ECPAC storms having the smallest asymmetry amplitude, at about 10%–15% of the azimuthal mean background. The TCs in ATL and SIND basins have larger asymmetry amplitudes, and the SIND is the extreme case with amplitudes up to 60% of the azimuthal mean background at a radius of 250 km.

c. Variability with TC intensity

The global composite shear-relative wavenumber-1 asymmetry for all TCs (Fig. 4a) and for three different TC intensity groups (Figs. 4b–d) were constructed by mirroring the data from the Southern Hemisphere around the shear direction to account for the Coriolis effect. The rainfall maximum is downshear left in the inner 200 km, and shifts toward the shear direction at larger radii from the TC center. The asymmetry amplitude increases with the radial distance, from being nearly zero near the center to 40% of the azimuthal mean rain rate by the 200-km radius. Although the wavenumber-2 asymmetry is also computed (not shown), the amplitude is only half of the wavenumber-1 asymmetry. So we will only focus on the wavenumber-1 asymmetry in this study.

For the stratification by TC intensity, 915 TRMM observations are available for TS, 451 for CAT12, and

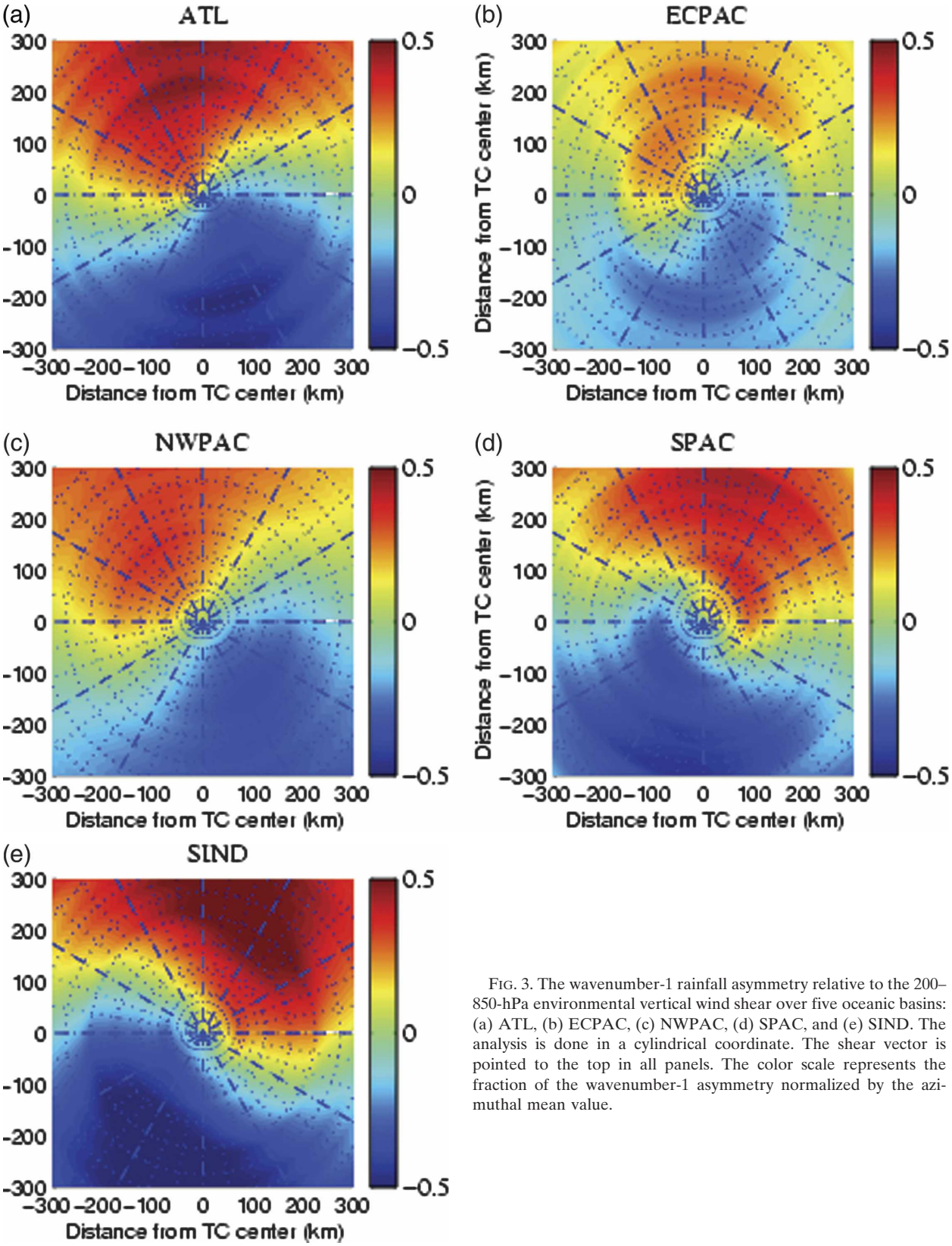

FIG. 3. The wavenumber-1 rainfall asymmetry relative to the 200–850-hPa environmental vertical wind shear over five oceanic basins: (a) ATL, (b) ECPAC, (c) NWPAC, (d) SPAC, and (e) SIND. The analysis is done in a cylindrical coordinate. The shear vector is pointed to the top in all panels. The color scale represents the fraction of the wavenumber-1 asymmetry normalized by the azimuthal mean value.

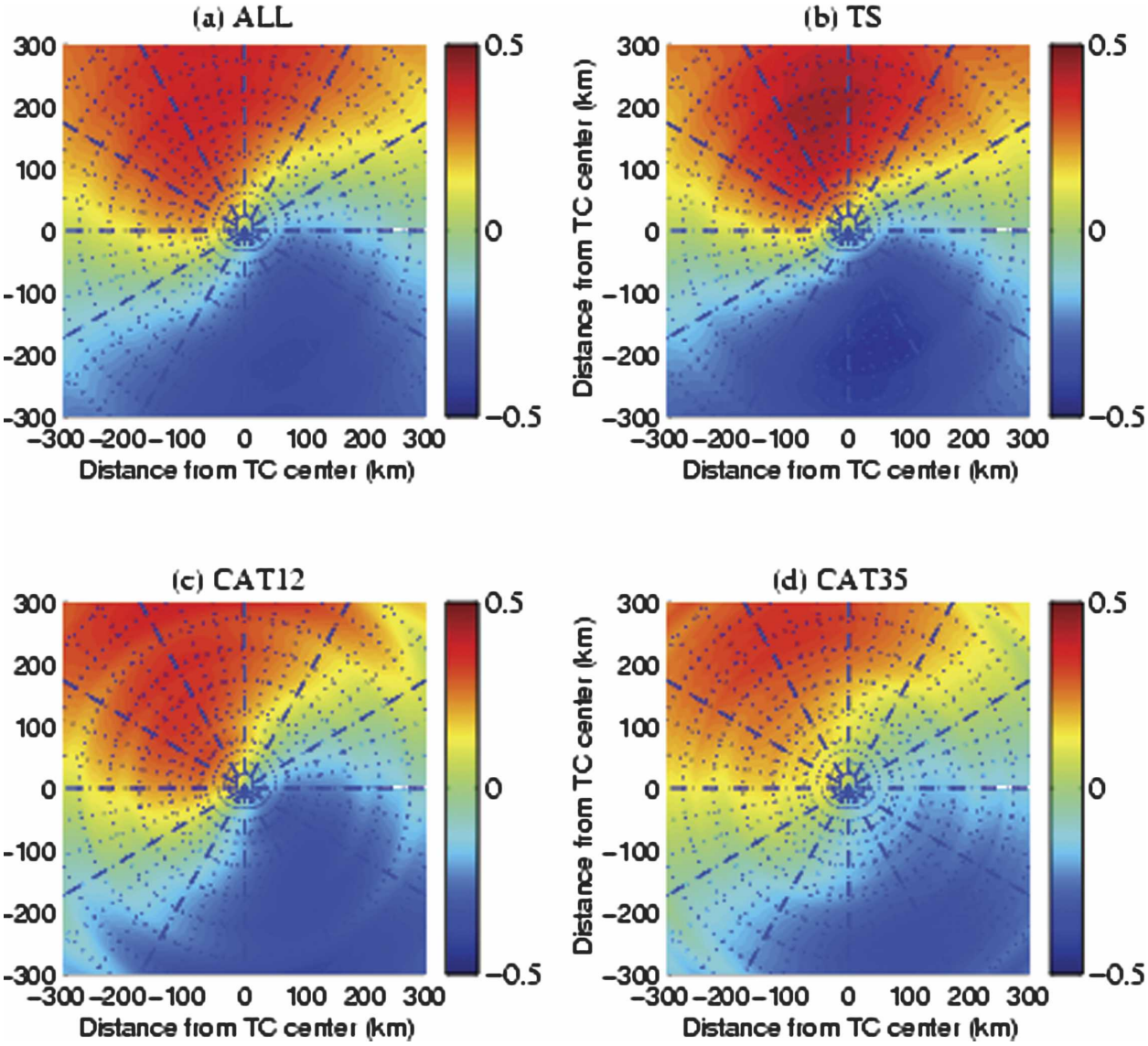

FIG. 4. Same as in Fig. 3, but for various TC intensity groups: (a) all TCs average, (b) TS, (c) CAT12, and (d) CAT35.

168 for CAT35, respectively. These numbers correspond to 60%, 29%, and 11% of all observations, respectively. The dataset used in this study is smaller than that in LMC, because of the lack of collocated shear data over some of the TRMM TC observations. The maximum of the wavenumber-1 rainfall asymmetry is downshear or downshear left for all TC intensity groups. As the TC intensity increases, the asymmetry shifts cyclonically to the left, especially within the inner 200-km radius from the TC center. Farther from the storm center, the asymmetry maximum has a greater downshear component. The amplitude of the rainfall asymmetry decreases with increasing TC intensity, which indicates that as storms intensify the stronger tangential wind advects the rainfall azimuthally farther around the storm.

Some of the basin variability in the rainfall asymmetry shown in Fig. 3 may be related to differences in the sampling of TCs in each of the intensity groups in various basins. As shown in LMC, the ATL database is biased toward the CAT12 and CAT35 systems, which account for 52% of the ATL observations, whereas they account for 39.5%, 35%, 30%, and 35% in NWPAC, ECPAC, SPAC, and SIND, respectively. Despite this sampling difference, asymmetries in ATL and NWPAC in Fig. 3 are comparable. The SH basins display the largest asymmetries, even though the distributions of TCs intensity are most similar to those in ECPAC.

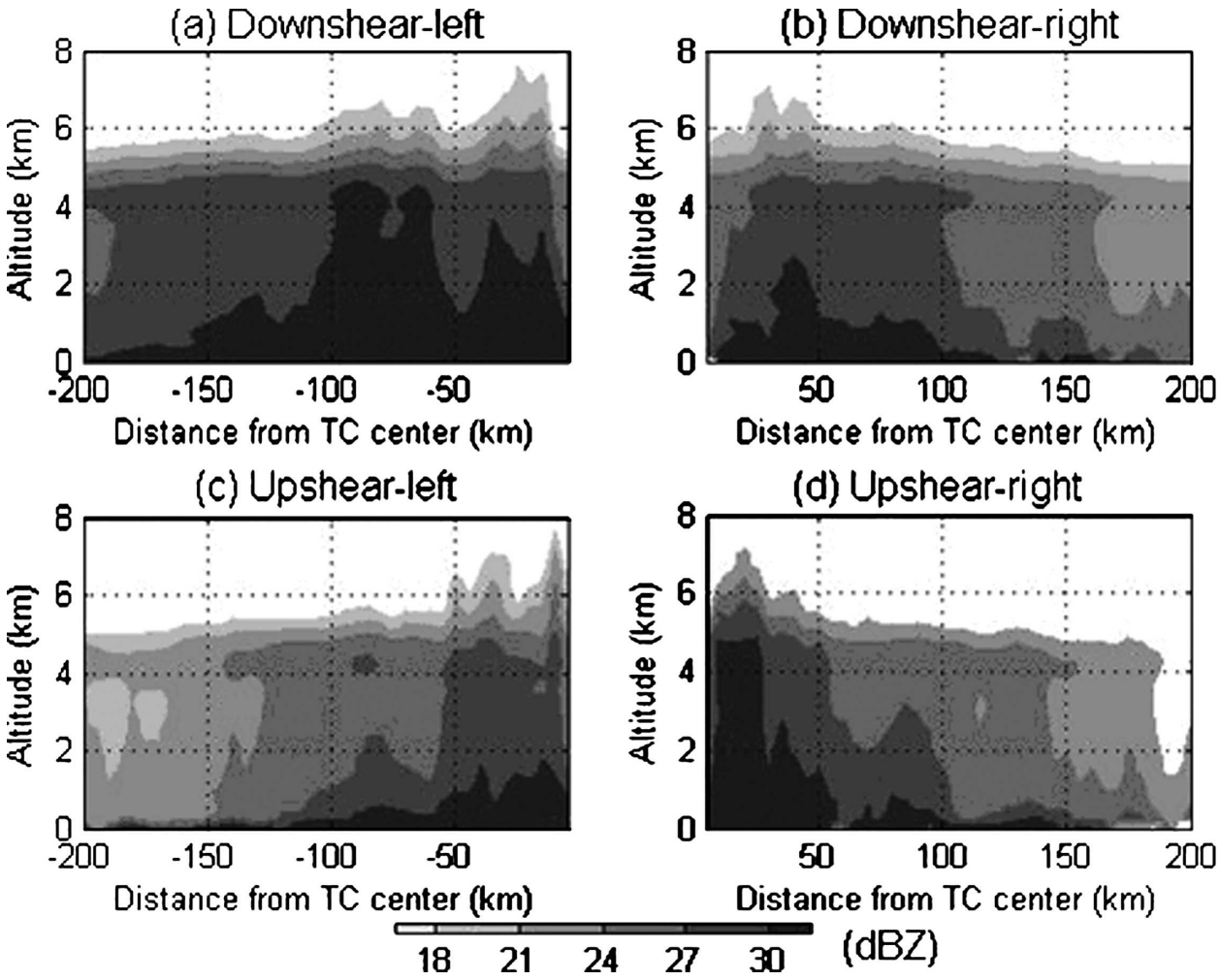

FIG. 5. (a)–(d) The shear-relative quadrant composites of the TRMM PR reflectivity (dBZ) for all TCs.

d. Vertical structure of the asymmetry

The TRMM PR reflectivity data provide a unique opportunity to examine the vertical structure of the precipitation asymmetry in terms of the shear-relative quadrant composites of TRMM PR reflectivity (Fig. 5). The largest reflectivity values are generally observed in the downshear-left quadrant (Fig. 5a), which is consistent with the TMI rainfall estimates shown in Fig. 4a. The relatively large value of reflectivity within the 50-km radii in the upshear-right quadrant (Fig. 5d) may be unrealistic due to the uncertainty of the storm center position in some cases. The shear effect is observed through the entire depth of the storm, which indicates that the convection is asymmetrically reorganized in the presence of shear. This observation is consistent with the numerical modeling studies of Frank and Ritchie (1999, 2001) in which they simulated the asymmetry in the vertical motion and cloud fields in response to an imposed vertical wind shear.

e. Asymmetry varying with shear strength

To explore whether the rainfall asymmetry variability in Figs. 4 and 5 is related to the shear magnitude, the frequency of occurrence for each of the TC intensity groups and for five oceanic basins are shown in Fig. 6. More CAT35 systems occur in the relatively low shear environment than do tropical storms (Fig. 6a), and the ECPAC TCs occur in the lowest mean shear environment (Fig. 6b). The mean shear amplitude in ECPAC is 5.7 m s^{-1}. All other basins have similar shear distributions, with a mean shear around 8.5 m s^{-1} and some TCs existing in relatively high shear conditions, up to 15–20 m s^{-1}. The decreasing mean vertical wind shear with increasing TC intensity (from 8.4 m s^{-1} for TS, to 7.7 and 6.2 m s^{-1} for CAT12 and CAT35, respectively) is consistent with the vertical shear being a limiting factor in TC development and intensification.

The effect of shear strength on the spatial distribution of rainfall can be demonstrated by partitioning TCs

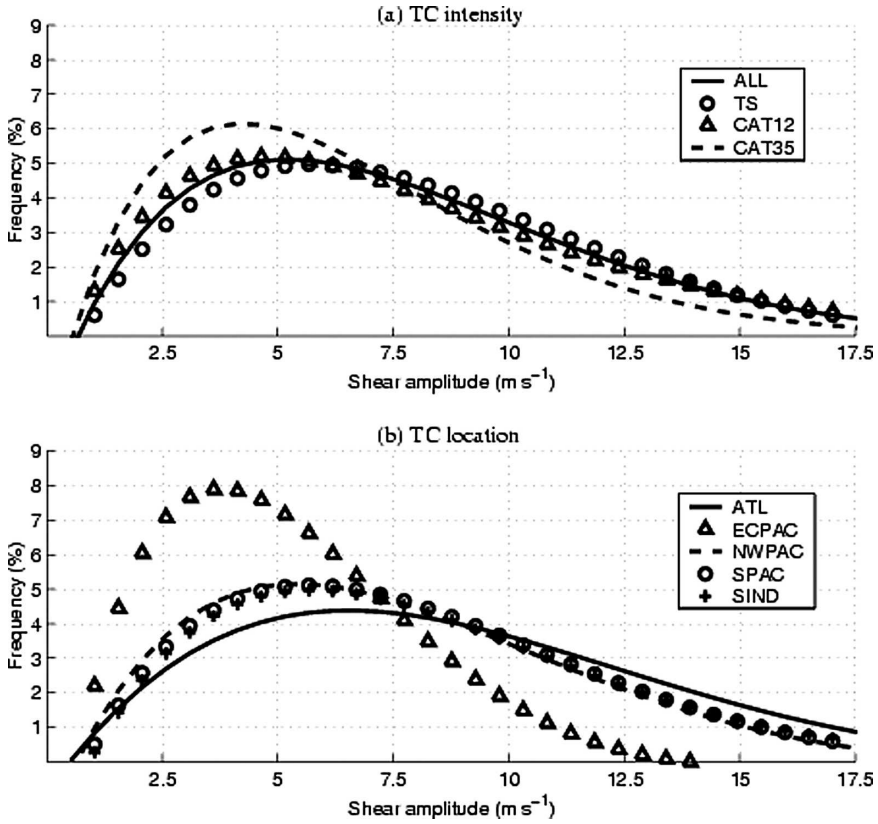

FIG. 6. Probability density functions of SHIPS and STIPS shear estimates at the time of TRMM observations, with respect to (a) TC intensity and (b) TC location.

into three subsets with shear values <5, 5–7.5, and >7.5 m s^{-1} based on the TC-shear distribution in Fig. 6a. The frequency peak is around 5 m s^{-1} in most cases. The wavenumber-1 rainfall asymmetry with respect to TC intensity for the three shear groups is shown in Fig. 7. A striking increase in asymmetry amplitude occurs as the shear exceeds 7.5 m s^{-1}. This increase in rainfall asymmetry is observed for all TC intensity groups. For TCs in moderate shear of 5–7.5 m s^{-1}, the maximum asymmetry is still downshear left, but with only half the magnitude compared to that of strong shear. When the shear is <5 m s^{-1}, the asymmetry does not have a dominant downshear-left pattern; rather the asymmetry is mostly downshear.

4. Combined effect of TC motion and wind shear on rainfall asymmetry

a. Global composite

The TC translation speed is known to affect the circulation around the TC through enhanced low-level convergence in the front quadrants (Shapiro 1983), which can induce a front to front-right rainfall asymmetry, as was shown by LMC. The magnitude of the rainfall asymmetry was found to be twice as large for the fast TCs (translation speed >5 m s^{-1}) compared with that in the relatively slow moving TCs (see Fig. 19 of LMC).

The global distribution of TC translation speed and direction is shown in Fig. 8 using the best-track database from NHC and JTWC over the period from 1949 to 2003. In the tropical belt between 20°S and 20°N, most TCs have a translation speed below 5 m s^{-1}. Some exceptions occur in the eastern Atlantic and, to a lesser extent, the central Pacific where relatively higher average translation speeds are observed, because of the stronger easterly flow in these regions. The translation speeds increase with latitude from about 7.5 m s^{-1} between 20° and 30° latitudes to 10–15 m s^{-1} or higher poleward of 30° latitude. The TC tracks are generally westward within 15° of the equator, except in NIND and the marginal seas and gulfs (e.g., the South China Sea and the eastern Caribbean Sea–Gulf of Mexico). For the remaining latitudes, storm motions acquire a poleward component on average. The corresponding distribution for the 1998–2000 period of this study (Fig. 8b) has the general features of the long-term mean shown in Fig. 8a, except the data are sparse in some

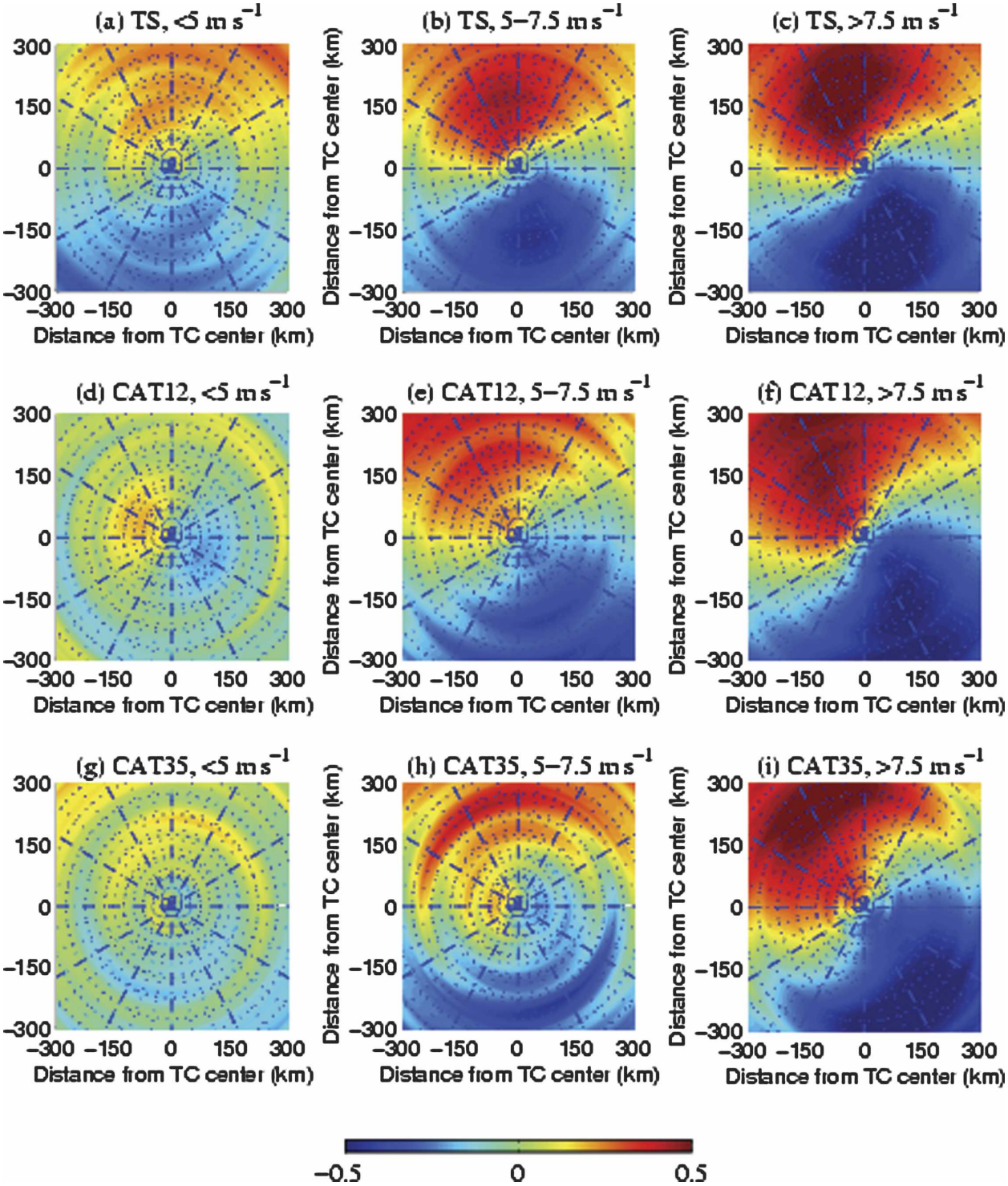

FIG. 7. Same as in Fig. 3, but for various shear magnitudes: TS, shear (a) <5, (b) 5–7.5, (c) >7.5 m s^{-1}; CAT12, shear (d) <5, (e) 5–7.5, and (f) >7.5 m s^{-1}; and CAT35, shear (g) <5, (h) 5–7.5, and (i) >7.5 m s^{-1}.

regions. The TCs in ECPAC are slightly faster during 1998–2000 than in the long-term mean.

Although the composites of TC rainfall asymmetry have been done either relative to shear vector in this study or relative to TC motion direction in LMC, the rainfall asymmetry observations ultimately include the combined effects of the shear and TC motion. In many ways, TC motion is not independent of the environ-

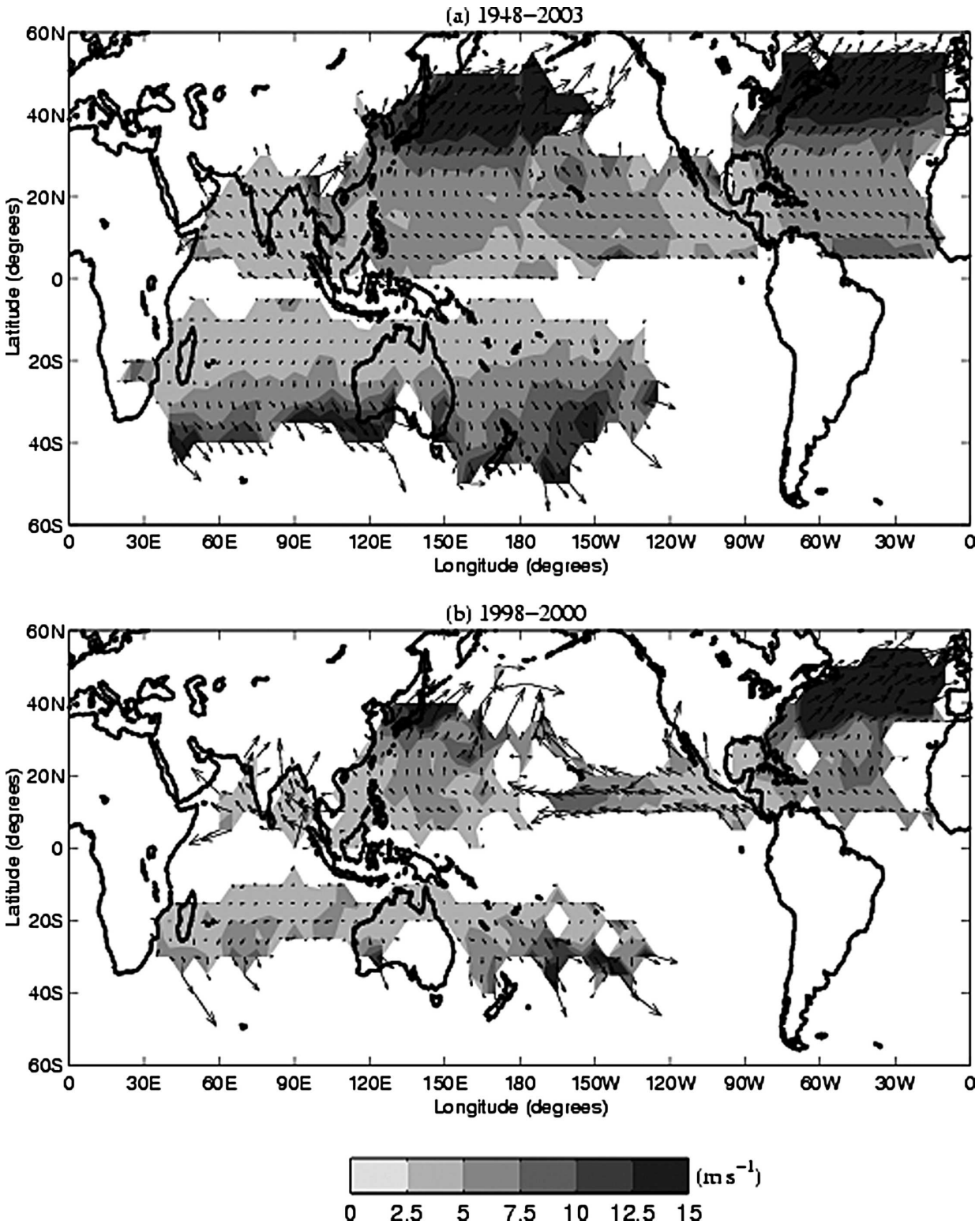

FIG. 8. Global maps of TC motion direction and translation speed calculated from the best track (HURDAT and JTWC) databases for (a) 1949–2003 and (b) 1998–2000.

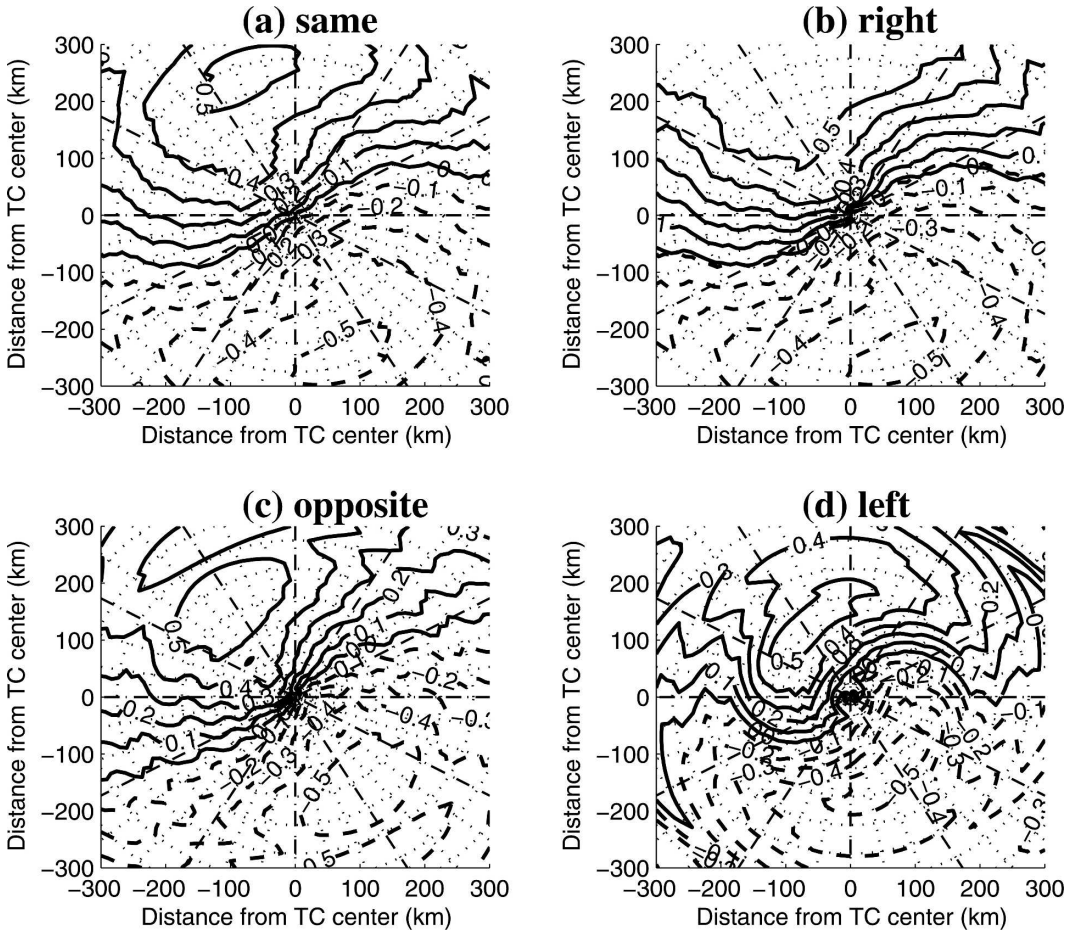

FIG. 9. The shear-relative wavenumber-1 rainfall asymmetry in strong shear (>7.5 m s^{-1}) for (a) shear and TC motion are in the same direction, (b) shear to the right of motion, (c) shear and motion are in the opposite direction, and (d) shear to the left of motion. The shear vector is pointed to the top of each panel. The contour value represents the fraction of the wavenumber-1 asymmetry normalized by the azimuthal mean.

mental shear. To further examine how the two factors affect the TC rainfall asymmetry, the cases are grouped such that the shear vectors are in the same, opposite, right, or left of the TC motion directions, and by the strength of the shear value, as shown in Figs. 9 and 10. In the strong shear (>7.5 m s^{-1}) environment (Fig. 9), the TC rainfall asymmetry seems to be governed more by the shear-induced effect than the motion-induced effect. All cases in Fig. 9 display a dominant downshear-left asymmetry maximum regardless of the TC motion relative to the shear. When the shear vector is 90° to the right of the storm motion vector, the combined motion-relative (front right) and shear-relative (downshear left) components result in the largest rainfall asymmetry (Fig. 9b). When the TC motion is opposite of the shear vector, the maximum rainfall asymmetry is only shifted slightly (Figs. 9a,c). One of the reasons for the relatively small changes from the case in Figs. 9a–c is that the TCs tend to move slower when the strong shear is against TC motion. The mean translation speed is 5.7 m s^{-1} when the shear and motion vectors are in the same direction, whereas it decreases to 4.2 m s^{-1} when the two vectors are in the opposite direction.

In the low-shear environment (Fig. 10), the TC motion may become a more important factor. The wavenumber-1 rainfall asymmetry shows an interesting variation in the radial distribution (Fig. 10). In the inner-core region (within the 150-km radius of the TC center), the rainfall asymmetry maximum is downshear left for all cases, and varies only slightly with the TC motion vector relative to the shear vector. The rainfall in the outer region is more sensitive to the TC motion, which is consistent with the low-level convergence due to the TC motion. The wavenumber-1 asymmetry in the outer region tends to be in the front and front-right

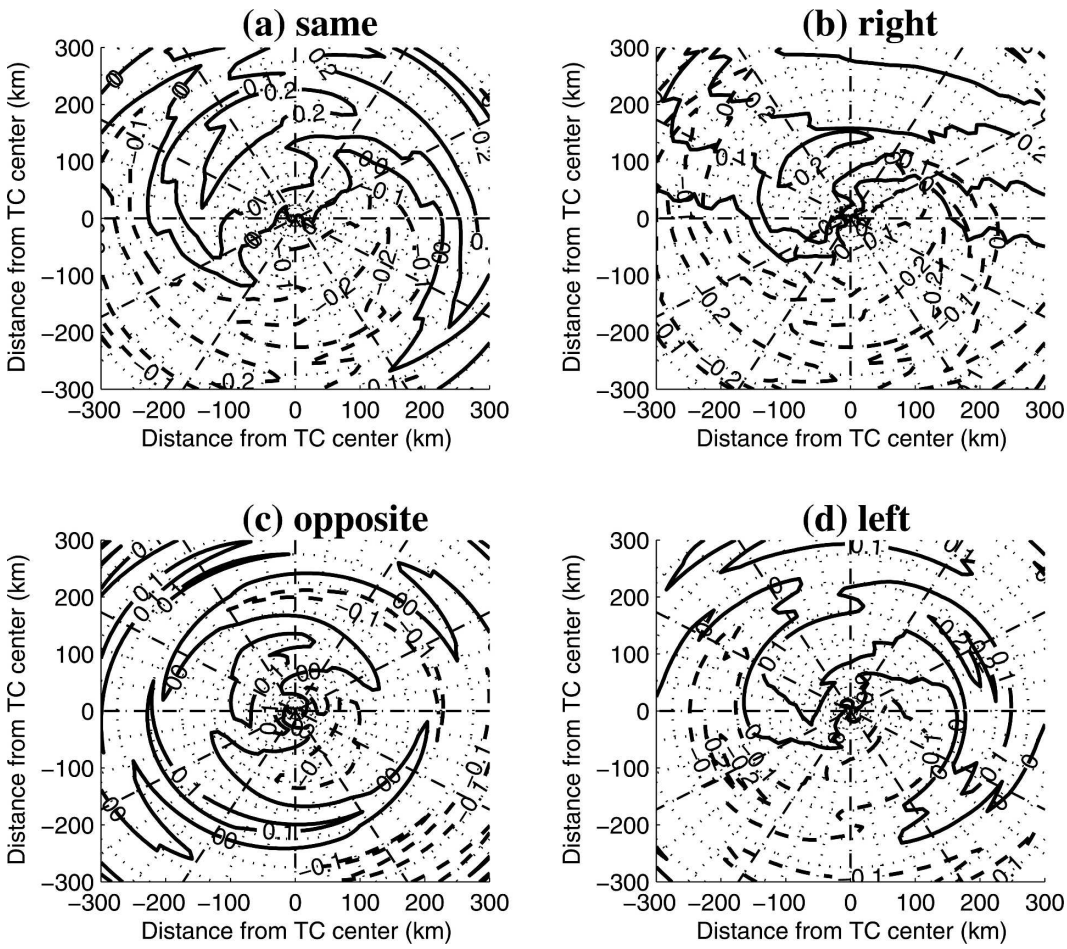

FIG. 10. Same as in Fig. 9, but for a relatively weak shear environment (<5 m s^{-1}).

quadrants. When the shear and motion vectors are in the same direction, or the shear to the right of the motion, the asymmetry is relatively large. In these two cases, the combination of motion-induced front and front right and the shear-induced downshear-left components creates a favorable overlap ahead of TCs (Figs. 10a,b). When the shear and motion vectors are in opposite directions, or the shear to the left of the motion, the asymmetry is relatively small (Figs. 10c,d). The translation speeds in the first two cases (Figs. 10a,b) are generally faster than that in the latter two cases (Figs. 10c,d), which may be a factor contributing to the difference in the amplitudes of the rainfall asymmetry.

The numerical simulation of Hurricane Bonnie (in 1998) by Rogers et al. (2003) showed similar rainfall asymmetry patterns to those of the composites in Figs. 10a,b. The shear was initially strong and to the right of the storm track in Bonnie, which is similar to the situation shown in Fig. 9b, when the largest rainfall asymmetry was observed. The shear later weakened and became along-track, which is similar to Fig. 10a, and the rainfall became more symmetric before the landfall. Although the shear along a storm track may vary with time, the TRMM-observed instantaneous rainfall asymmetry can still provide valuable information at a given time.

b. Ocean basin variability

The global environmental vertical wind shear and TC motion vary from basin to basin as shown in Figs. 1 and 8. Similar to Fig. 7, TC motion variability can be summarized using the PDF of the translation speed in Fig. 11. Although the TC translation speeds vary only slightly for different TC intensity groups (Fig. 11a), a significant variability is observed for different oceanic basins (Fig. 11b). Translation speeds are relatively slower in SPAC and SIND than in the other basins, while TCs in ATL are faster than most. The question is how these variabilities affect the TC rainfall asymmetry in different ocean basins?

The rainfall variability due to the combined effect of TC motion and vertical wind shear is presented in Figs.

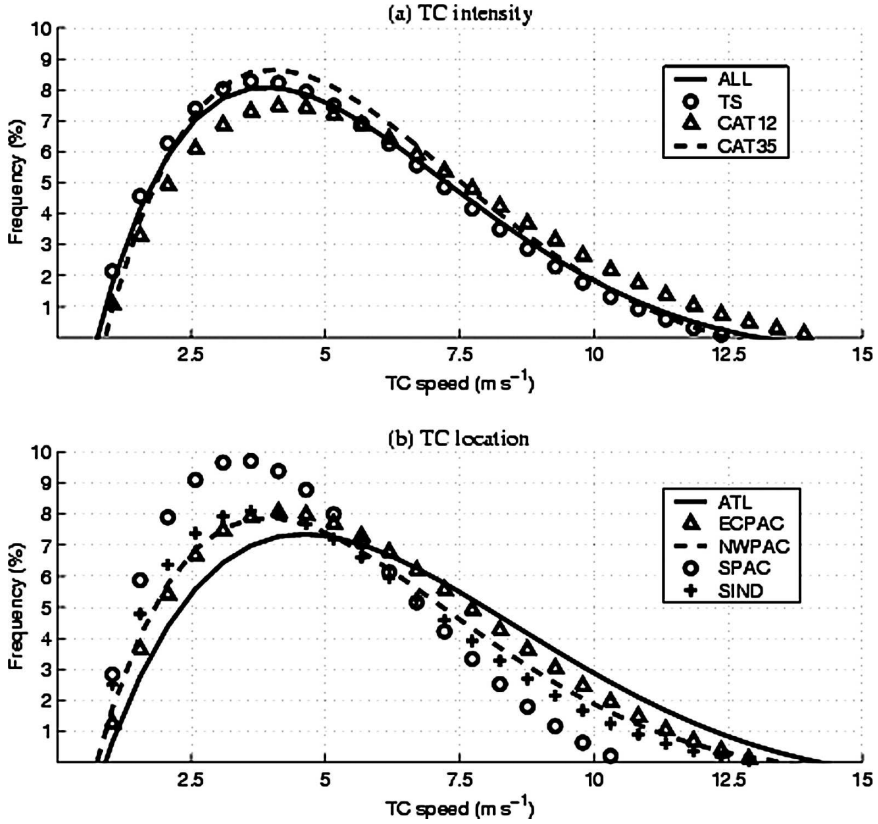

FIG. 11. Probability density functions of TC translation speeds at the time of TRMM observations, with respect to (a) TC intensity and (b) TC geographical location.

12 and 13. The motion-relative rainfall asymmetries for all ocean basins[1] have been shown in LMC, which is adopted in Fig. 12 for easy comparison, except in the NIND where the number of TRMM observations collocated with the shear data is very limited. This motion-relative composite of rainfall asymmetry does not exclude the effect of wind shear. To better represent the contributions from both the TC motion and wind shear, we compute the relative position of the storm track and shear vector for all TCs in each oceanic basin. The angular distribution in eight 45° bins of the occurrence of shear vector relative to the TC propagation direction by oceanic basins is shown in Fig. 13. In ATL and NWPAC, shear vectors are most likely to the right of the TC track, whereas in SH (SPAC and SIND), the opposite occurs with the shear preferentially pointing to the left of the TC track. The largest TC rainfall asymmetry is observed in ATL and SIND (Figs. 12a,e) where the shear vectors are most likely to be at 90° to the either the left or right of the TC tracks (Fig. 13). The TCs in ECPAC have a very different TC motion and shear distribution, with shear frequently occurring to the left but close to the TC motion direction, compared to that in other basins. The TC environmental shear is also relatively weak in ECPAC (Fig. 6b).

The PDFs for the shear and TC translation speeds in Figs. 6b and 11b indicate that the TCs in ATL move relatively faster and have higher shear than those in other basins. Both the ATL and NWPAC include many northward-recurving TCs near the coastal regions. These results are consistent with those in Corbosiero and Molinari (2003), who found that the TC motion in the Atlantic is related to the orientation of the shear primarily due to the downshear shift of the upper-tropospheric anticyclone. The asymmetry was likely the result of the superposition of the shear and motion vectors. As indicated above, the magnitude of the vertical wind shear is a primary factor affecting TC rainfall asymmetry when the shear is strong. However, when the shear is relatively weak, the TC motion becomes a relatively important factor in the rainfall asymmetry,

[1] Note that in LMC, the "%" symbol in Figs. 9 and 17–19 should be removed. The asymmetry is normalized to the azimuthal average and a value of 0.3 means 30%.

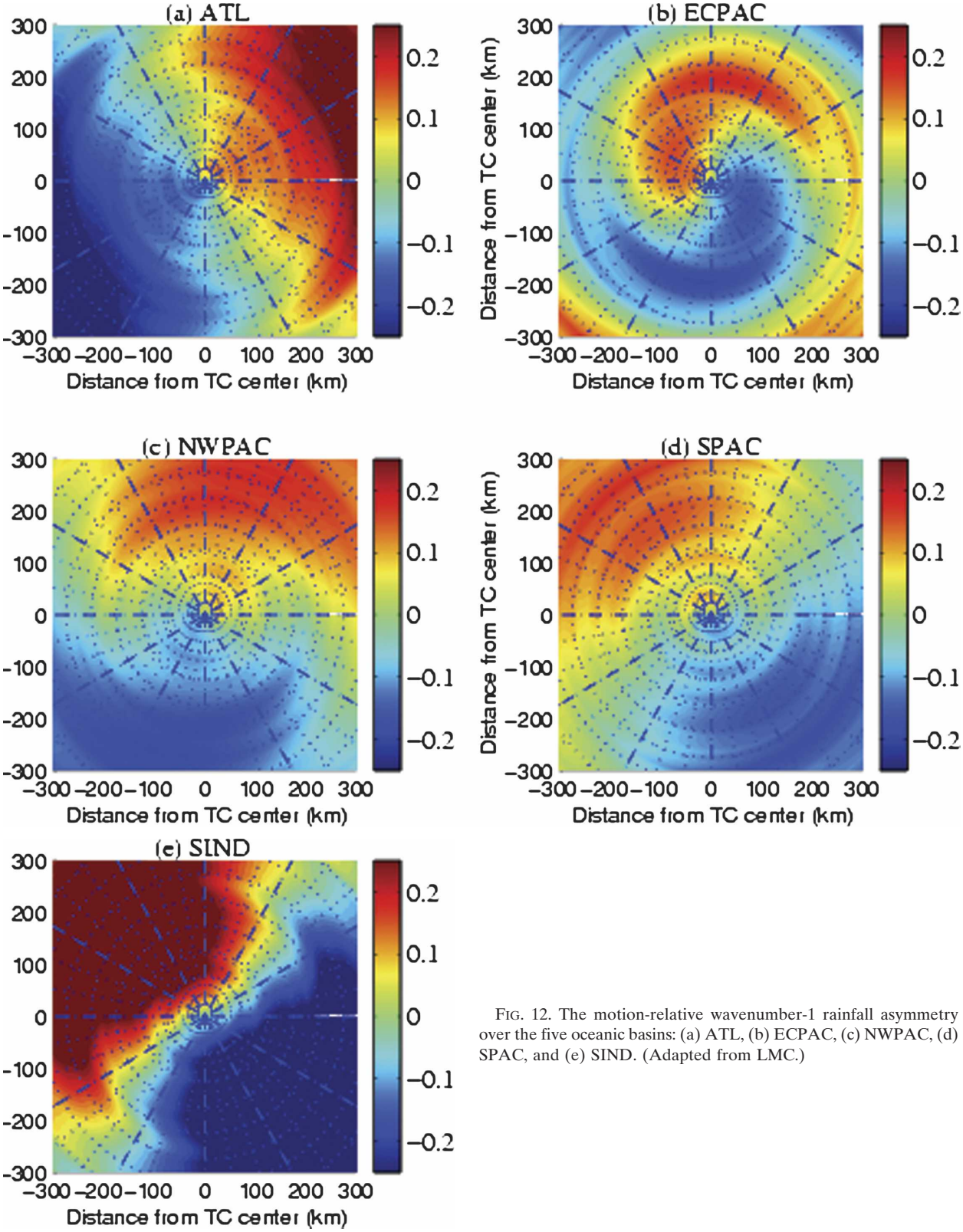

FIG. 12. The motion-relative wavenumber-1 rainfall asymmetry over the five oceanic basins: (a) ATL, (b) ECPAC, (c) NWPAC, (d) SPAC, and (e) SIND. (Adapted from LMC.)

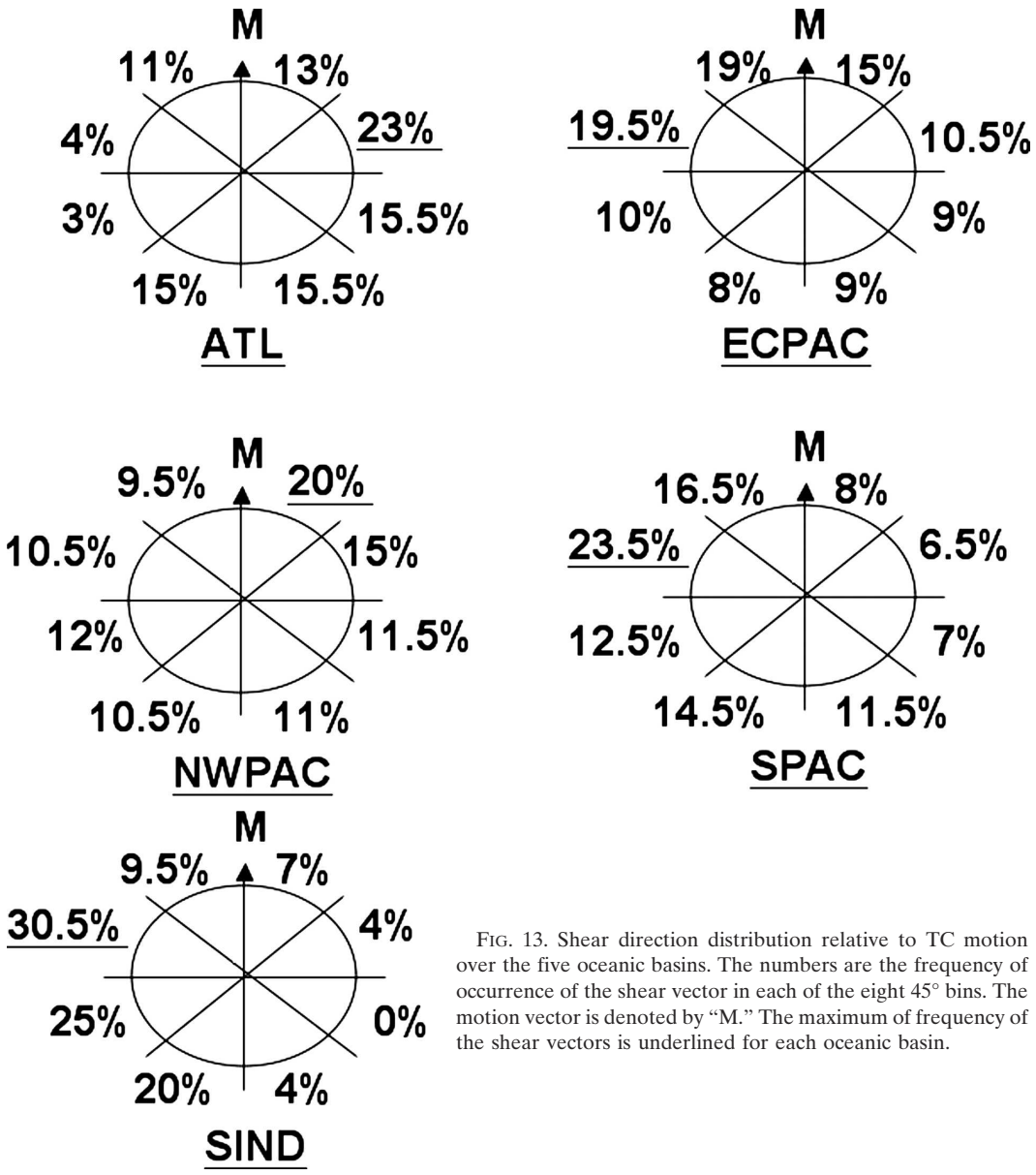

FIG. 13. Shear direction distribution relative to TC motion over the five oceanic basins. The numbers are the frequency of occurrence of the shear vector in each of the eight 45° bins. The motion vector is denoted by "M." The maximum of frequency of the shear vectors is underlined for each oceanic basin.

especially when the angle between TC motion and the shear vector is relatively small in ECPAC and NWPAC (Fig. 13).

5. Conclusions

The effect of environmental vertical wind shear on the TC rainfall structure is examined using the TRMM TMI rainfall estimates and the SHIPS and STIPS shear database over five oceanic basins. The spatial distribution is obtained by computing the Fourier coefficients for the first- and second-order rainfall asymmetry. The wavenumber-1 rainfall asymmetry maximum is mostly downshear left for all TC intensity groups and in all the Northern Hemisphere basins. In the Southern Hemisphere, the rainfall maximum is mostly downshear right consistent with the changing sign of the Coriolis parameter. The relative magnitude of the asymmetry decreases slightly as TC intensity increases. A large variability exists from basin to basin with the largest shear-relative rainfall asymmetry in the northern Atlantic and the south Indian Ocean (Fig. 3).

The results of the shear-relative analysis are compared with that for TC motion in LMC. A combined shear and TC motion analysis is conducted to examine the collective effect of the shear and motion on the TC rainfall asymmetry. In general, the TC rainfall asymmetry has larger amplitudes with respect to vertical

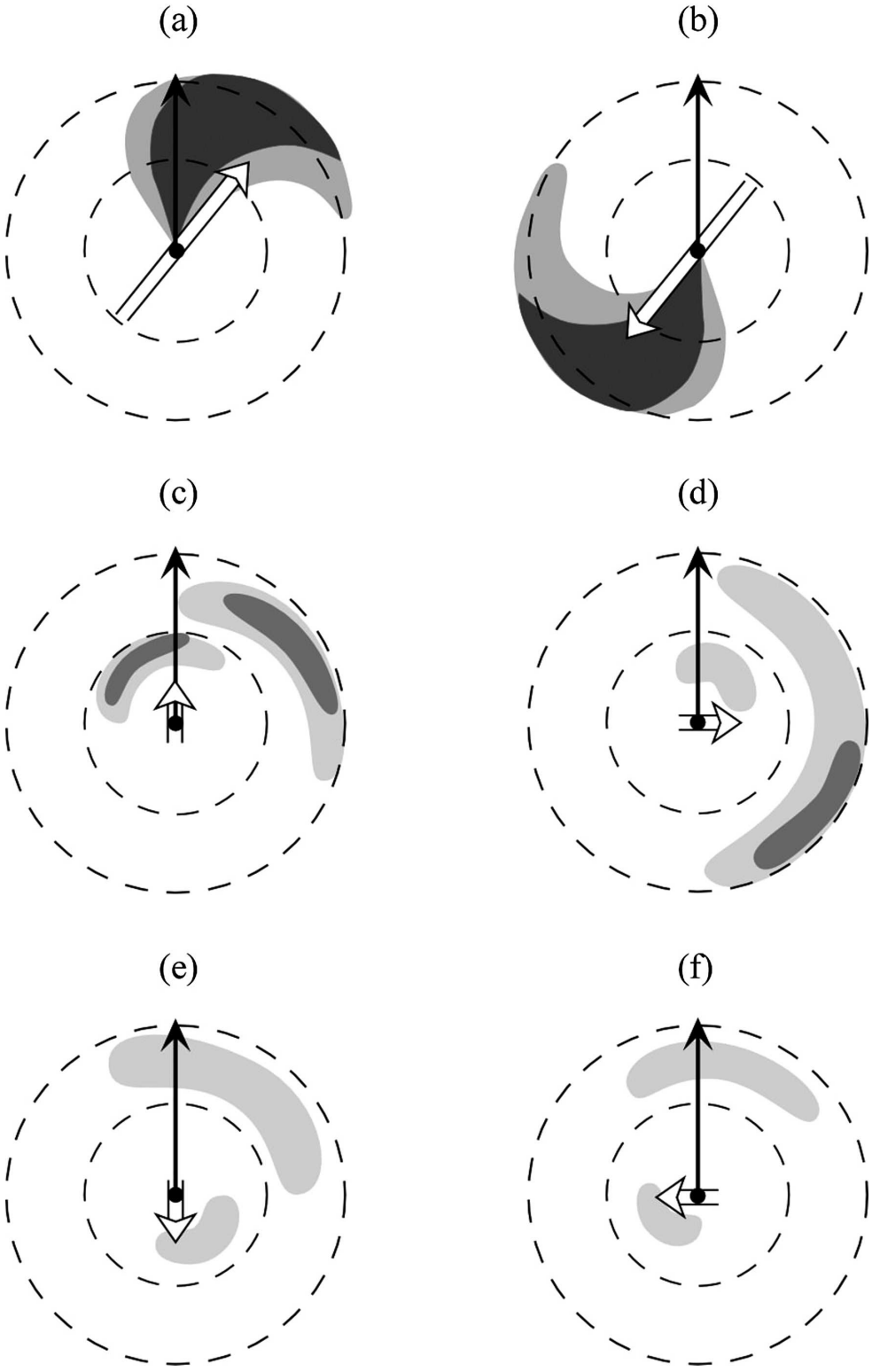

FIG. 14. Schematics illustrating the observed wavenumber-1 TC rainfall asymmetry (gray shading) in relation to the environmental vertical wind shear (wide white arrow) and TC motion (narrow black arrow) for the Northern Hemisphere. The length of the white arrow indicates the magnitude of shear. (a), (b) The strong shear environment (>7.5 m s^{-1}), where the shear is a dominant factor in determining the rainfall asymmetries. (c)–(f) The relatively weak shear environment, where the TC motion becomes more important in determining the rainfall asymmetries.

wind shear than to TC motion. In a moderate-to-strong shear environment, the rainfall asymmetry is predominately downshear left (Fig. 9). When the environment shear is weak, the TC motion–relative rainfall asymmetry has a larger contribution, especially in the outer rainband regions.

The simple schematics in Fig. 14 summarize the findings of this study. When the shear is strong (>7.5 m s^{-1}), the environmental shear is the dominant factor in determining the rainfall asymmetries that is largely downshear left, especially in the inner region (Figs. 14a,b). The TC translation speed and direction play an important role in the rainfall asymmetry when the shear is low (<5 m s^{-1}). In the low shear environment, the rainfall asymmetry is mainly ahead of the storm, especially in the outer rainband regions (Figs. 14c–f). However, the rainfall asymmetry with 100-km radius remains to be downshear left. The magnitude of the asymmetry is determined by the juxtaposition of the shear and motion vectors, with the largest asymmetry when the two vectors are in the same direction (Fig. 14c).

This study provides some new insights on the TC rainfall asymmetry in relation to the environmental vertical wind shear and motion in various global TC basins. It also provides a useful conceptual model for operational applications of TC rainfall forecasting over the different oceanic basins around the globe. Although we cannot fully explain the dynamic processes associated with the vertical wind shear that affect the TC rainfall structure, especially the convection in both inner core and outer rainband regions, more comprehensive numerical modeling study using a high-resolution, cloud-resolving model is in progress to better understand the physical mechanisms responsible for the observed TC rainfall asymmetry.

Acknowledgments. We thank Dr. Molinari and two anonymous reviewers whose critical and valuable comments and suggestions have helped to improve the manuscript. We also thank Joe Tenerelli, John Cangialosi, and Derek Ortt for their assistance during the course of this study. This study is supported by an NSF Grant ATM9908944, a NOAA Grant NA17RJ1228, and NASA Grants NAG5-10963 and NNG04GK05G.

REFERENCES

Bender, M. A., 1997: The effect of relative flow on the asymmetric structure in the interior of hurricanes. *J. Atmos. Sci.,* **54,** 703–724.

Black, M. L., J. F. Gamache, F. D. Marks Jr., C. E. Samsury, and H. E. Willoughby, 2002: Eastern Pacific Hurricanes Jimena of 1991 and Olivia of 1994: The effect of vertical shear on structure and intensity. *Mon. Wea. Rev.,* **130,** 2291–2312.

Burpee, R. W., and M. L. Black, 1989: Temporal and spatial variations of rainfall near the centers of two tropical cyclones. *Mon. Wea. Rev.,* **117,** 2204–2218.

Corbosiero, K. L., and J. Molinari, 2003: The relationship between storm motion, vertical wind shear, and convective asymmetries in tropical cyclones. *J. Atmos. Sci.,* **60,** 366–376.

DeMaria, M., 1996: The effect of vertical wind shear on tropical cyclone intensity change. *J. Atmos. Sci.,* **53,** 2076–2087.

——, and J. Kaplan, 1994: A statistical hurricane intensity prediction scheme (SHIPS) for the Atlantic basin. *Wea. Forecasting,* **9,** 209–220.

——, and ——, 1999: An updated statistical hurricane intensity prediction scheme (SHIPS) for the Atlantic and eastern North Pacific basins. *Wea. Forecasting,* **14,** 326–337.

Desflots, M., and S. S. Chen, 2004: A numerical study of rapid intensity change in Hurricane Lili (2002). Preprints, *26th Conf. on Hurricanes and Tropical Meteorology,* Miami, FL, Amer. Meteor. Soc., 574–575.

Dunion, J. P., and C. S. Velden, 2004: The impact of the Sahara air layer on Atlantic tropical cyclone activity. *Bull. Amer. Meteor. Soc.,* **85,** 353–365.

Dvorak, V. F., 1984: Tropical cyclone intensity analysis using satellite data. NOAA Tech. Rep. NESDIS 11, Washington, DC, 46 pp.

Elsberry, R. L., and R. A. Jefferies, 1996: Vertical wind shear influences on tropical cyclone formation and intensification during TCM-92 and TCM-93. *Mon. Wea. Rev.,* **124,** 1374–1387.

Emanuel, K. A., 1988: The maximum intensity of hurricanes. *J. Atmos. Sci.,* **45,** 1143–1155.

——, 1997: Some aspects of hurricane inner-core dynamics. *J. Atmos. Sci.,* **54,** 1014–1026.

Frank, W. M., 1977: The structure and energetics of the tropical cyclone. Part I: Storm structure. *Mon. Wea. Rev.,* **105,** 1119–1135.

——, and E. A. Ritchie, 1999: Effects of environmental flow upon tropical cyclone structure. *Mon. Wea. Rev.,* **127,** 2044–2061.

——, and ——, 2001: Effects of environmental flow on the intensity and structure of numerically simulated hurricanes. *Mon. Wea. Rev.,* **129,** 2249–2269.

Hogan, T., and T. Rosmond, 1991: The description of the Navy Operational Global Atmospheric Prediction System's spectral forecast model. *Mon. Wea. Rev.,* **119,** 1786–1815.

Holland, G. J., 1997: The maximum potential intensity of tropical cyclones. *J. Atmos. Sci.,* **54,** 2519–2541.

Jarvinen, B. R., C. J. Neumann, and M. A. S. Davis, 1984: A tropical cyclone data tape for the North Atlantic Basin, 1886–1983: Contents, limitations, and uses. NOAA Tech. Memo. NWS NHC-22, 21 pp. [Available from NTIS, Technology Administration, U.S. Dept. of Commerce, Springfield, VA 22161.]

Jones, S. C., 1995: The evolution of vortices in vertical shear. I: Initially barotropic vortices. *Quart. J. Roy. Meteor. Soc.,* **121,** 821–851.

——, 2000a: The evolution of vortices in vertical shear. II: Large-scale asymmetries. *Quart. J. Roy. Meteor. Soc.,* **126,** 3137–3160.

——, 2000b: The evolution of vortices in vertical shear. III: Baroclinic vortices. *Quart. J. Roy. Meteor. Soc.,* **126,** 3161–3185.

——, 2004: On the ability of dry tropical-cyclone-like vortices to withstand vertical shear. *J. Atmos. Sci.,* **61,** 114–119.

Kalnay, E., and Coauthors, 1996: The NCEP/NCAR 40-Year Reanalysis Project. *Bull. Amer. Meteor. Soc.,* **77,** 437–471.

Knaff, J. A., J. P. Kossin, and M. DeMaria, 2003: Annular hurricanes. *Wea. Forecasting,* **18,** 204–223.

——, S. A. Seseske, M. DeMaria, and J. L. Demuth, 2004: On the influences of vertical wind shear on symmetric tropical cyclone structure derived from AMSU. *Mon. Wea. Rev.,* **132,** 2503–2510.

——, C. R. Sampson, and M. DeMaria, 2005: An operational statistical typhoon intensity prediction scheme for the western North Pacific. *Wea. Forecasting,* **20,** 688–699.

Kummerow, C., W. Barnes, T. Kozu, J. Shiue, and J. Simpson, 1998: The Tropical Rainfall Measuring Mission (TRMM) sensor package. *J. Atmos. Oceanic Technol.,* **15,** 809–817.

Lonfat, M., F. D. Marks Jr., and S. S. Chen, 2004: Precipitation distribution in tropical cyclones using the Tropical Rainfall Measuring Mission (TRMM) microwave imager: A global perspective. *Mon. Wea. Rev.,* **132,** 1645–1660.

Marks, F. D., Jr., 1985: Evolution of the structure of precipitation in Hurricane Allen (1980). *Mon. Wea. Rev.,* **113,** 909–930.

Marks, F. D., R. A. Houze Jr., and J. F. Gamache, 1992: Dual-aircraft investigation of the inner core of hurricane Norbert. Part I: Kinematic structure. *J. Atmos. Sci.,* **49,** 919–942.

Merrill, R. T., 1988: Environmental influences on hurricane intensification. *J. Atmos. Sci.,* **45,** 1678–1687.

Miller, B. I., 1958: Rainfall rates in Florida hurricanes. *Mon. Wea. Rev.,* **86,** 258–264.

Peng, M. S., and R. T. Williams, 1990: Dynamics of vortex asymmetries and their influence on vortex motion on a beta plane. *J. Atmos. Sci.,* **47,** 1987–2003.

——, B.-F. Jeng, and R. T. Williams, 1999: A numerical study on tropical cyclone intensification. Part I: Beta effect and mean flow effect. *J. Atmos. Sci.,* **56,** 1404–1423.

Rodgers, E. B., S. Chang, and H. F. Pierce, 1994: A satellite observational and numerical study of precipitation characteristics in western North Atlantic tropical cyclones. *J. Appl. Meteor.,* **33,** 129–139.

Rogers, R., S. S. Chen, J. Tenerelli, and H. Willoughby, 2003: A numerical study of the impact of vertical shear on the distribution of rainfall in Hurricane Bonnie (1998). *Mon. Wea. Rev.,* **131,** 1577–1599.

Shapiro, L. J., 1983: The asymmetric boundary layer flow under a translating hurricane. *J. Atmos. Sci.,* **40,** 1984–1998.